

Where are the binary source galactic microlensing events?

M. Dominik*

Institut für Physik, Universität Dortmund, D-44221 Dortmund, Germany

Received ; accepted

Abstract. Though there have been some galactic microlensing events which show a clear signature of a binary lens, no event has yet been claimed as due to lensing of a binary source. Here I argue that this may be due to the fact that most of the binary source events show light curves which can be fitted with the simpler model of a blended single source.

Key words: gravitational lensing — dark matter — Stars: low-mass, brown dwarfs — Galaxy: halo

1. Introduction

Among the galactic microlensing events detected by the 4 observing groups EROS (Aubourg et al. 1993), MACHO (Alcock et al. 1993, 1997a,b), OGLE (Udalski et al. 1994a-e), and DUO (Alard et al. 1995a,b), some events show the characteristics of a binary lens, namely MACHO LMC#1 (Dominik & Hirshfeld 1994, 1996), OGLE#7 (Udalski et al. 1994d), DUO#2 (Alard et al. 1995b), MACHO LMC#9 (Bennett et al. 1996), MACHO Bulge 95-12 (Pratt et al. 1995), and MACHO Bulge 96-3 (Stubbs et al. 1997). In contrast, no event has been claimed to involve a binary source, though Griest & Hu (1992) have predicted that around 10 % of the events should involve features of a binary source. Given this situation, one may clearly pose the question where the binary source microlensing events are.

Here I argue that the lack of claimed binary source microlensing events may be due to the fact that most of the light curves for such events can successfully be explained with the simpler model of a blended single source. In fact, such a model is successful for the event OGLE#5 (Dominik 1996; Alard 1997) and most of the DUO events also involve blending (Alard 1997). In this paper, I discuss also a model with a binary source for OGLE#5 and compare it with the model involving a blended single source.

2. Point-mass lens and point source

For a lens at a distance D_d from the observer, a source at a distance D_s from the observer, and D_{ds} the lens-source distance, the Einstein radius for a lens of mass M is given by

$$r_E = \sqrt{\frac{4GM}{c^2} \frac{D_d D_{ds}}{D_s}}. \quad (1)$$

Let the lens move on a straight line with a velocity v_\perp transverse to the line-of-sight observer-source, so that it moves one Einstein radius in the lens plane in the time $t_E = \frac{r_E}{v_\perp}$.¹ Let t_{\max} denote the time at the closest approach and $u_{\min} = r_{\min}/r_E$ the impact parameter at t_{\max} in units of Einstein radii. For the impact parameter at time t one obtains

$$u = \sqrt{u_{\min}^2 + [p(t)]^2}, \quad (2)$$

where

$$p(t) = \frac{t - t_{\max}}{t_E}. \quad (3)$$

The light amplification for a point source and a point-mass lens is given by

$$A_{SS}(u(t)) = \frac{u^2 + 2}{u\sqrt{u^2 + 4}}. \quad (4)$$

3. Point-mass lens and binary source

For a binary source, according to Griest & Hu (1992), two values of t_{\max} and u_{\min} defining the closest approach to the first and to the second source object are used, which imply two functions $u_1(t)$ and $u_2(t)$. With L_1 and L_2 being the luminosities of the two parts and the luminosity offset ratio

$$\omega = \frac{L_2}{L_1 + L_2}, \quad (5)$$

the light amplification is given by

$$A_{BS}(u_1(t), u_2(t)) = (1 - \omega)A_{SS}(u_1) + \omega A_{SS}(u_2), \quad (6)$$

¹ Note that this is equivalent to letting the source projected onto the lens plane move with v_\perp into the opposite direction. Further note that if the fixed source is on the right side of the lens trajectory, a corresponding fixed lens is on the right side of the source trajectory.

* Present address: Space Telescope Science Institute, 3700 San Martin Drive, Baltimore, MD 21218, USA (dominik@stsci.edu)

so that the light curve is a superposition of two light curves for point sources behind point-mass lenses.

Since the two components of the binary source may be located on the same side or on opposite sides of the lens trajectory without changing the distance functions $u_1(t)$ and $u_2(t)$, two different physical configurations producing the same light curve exist. I call the case where the components are on the same side the *cis*-configuration, the case where the components are on opposite sides the *trans*-configuration.

Let 2ρ denote the distance between the closest approaches of the lens to the two components and 2λ denote the distance between the source components, both measured in projected Einstein radii $r'_E = \frac{D_s}{D_d} r_E$. It follows that

$$\rho = \frac{t_{\max,2} - t_{\max,1}}{2t_E}. \quad (7)$$

The angle β between the direction from source component 1 to source component 2 and the lens trajectory is given by

$$\begin{aligned} \beta &= \arctan \frac{u_{\min,2} \pm u_{\min,1}}{2\rho} \\ &= \arctan \left(\frac{u_{\min,2} \pm u_{\min,1}}{t_{\max,2} - t_{\max,1}} t_E \right), \end{aligned} \quad (8)$$

where the upper sign refers to the *trans*-configuration and the lower sign refers to the *cis*-configuration. The half-distance between the components follows as

$$\lambda = \rho / \cos \beta. \quad (9)$$

4. Comparison of binary source and blended single source

In contrast to the light amplification for a binary source (Eq. (6)), one obtains for a blended single source

$$A_{\text{blend}} = f A_{\text{SS}}(u) + 1 - f, \quad (10)$$

where the blending parameter f gives the contribution of the light of the source at unlensed state to the total light (source and component which does not undergo any lensing).

In the case of large u_1 , one has $A_{\text{SS}}(u_1) \approx 1$ and therefore

$$A_{\text{BS}}(u_1(t), u_2(t)) \approx 1 - \omega + \omega A_{\text{SS}}(u_2), \quad (11)$$

i.e. the light curve for a binary source approaches that for a blended single source (object 2), and $\omega \approx f$, where the blended single source is the exact limit of the binary source for $u_1 \rightarrow \infty$. Similarly, for large u_2 , one has $A_{\text{SS}}(u_2) \approx 1$ and

$$A_{\text{BS}}(u_1(t), u_2(t)) \approx (1 - \omega) A_{\text{SS}}(u_1) + \omega, \quad (12)$$

so that one approaches the light curve for a blended single source which now is object 1, and $\omega \approx 1 - f$. For $u = 2$, one obtains $A_{\text{SS}} = \frac{3}{2\sqrt{2}} \approx 1.06$, so that for $u_{\min,1} \geq 2$ ($u_{\min,2} \geq 2$), the light curves for a blended single source object 2 (1) and for a binary source differ by less than 6%. This shows that *any* blended event will have a successful fit with a binary source, where large uncertainties in some of the fit parameters are expected, because the binary source model involves more

parameters than that for a blended single source, namely for n spectral bands the distance parameter $u_{\min,1}$ ($u_{\min,2}$), the point of time $t_{\max,1}$ ($t_{\max,2}$) and the luminosity offset ratios ω_i (altogether $n + 2$ parameters) are convolved into n blending parameters f_i .

Griest & Hu (1992) have performed a comprehensive study on the types of events which arise for binary sources. Depending on the type of the primary star of the binary system and the lens mass, they find that among the binary source events, 60–95% have a light curve which is mainly effected by one of the objects only. They call these events “offset bright” event if this object is the brighter one and “offset dim” or “merged offset dim” of this object is the dimmer one², where 50–80% of the binary source events fall into the category “offset bright”, 7–20% into the category “offset dim” and 0.3–2% into the category “merged offset dim”. The large fraction of these types of events among the binary source events means that it is likely that events due to binary sources can be successfully fitted with the model of a blended single source.

5. OGLE#5 as an example

The points mentioned above can be illustrated using the event OGLE#5 as an example. Table 1 shows the result of a fit for a single source with and without blending, while Table 2 shows the result of a fit with a binary source.

Table 1. OGLE #5: Fits for a single source with and without blending

parameter	no blending	blending
t_E [d]	12.48 ^{+0.36} _{-0.36}	62 ⁺¹⁴ ₋₁₀
t_{\max} [d]	824.331 ^{+0.017} _{-0.017}	824.36 ^{+0.018} _{-0.017}
u_{\min}	0.0848 ^{+0.0013} _{-0.0013}	0.0137 ^{+0.0027} _{-0.0025}
m_{base}	-17.904 ^{+0.011} _{-0.011}	-17.960 ^{+0.012} _{-0.013}
f	—	0.166 ^{+0.032} _{-0.030}
χ_{\min}^2	361.00	117.93
# d.o.f = n	97	96
$\sqrt{2\chi_{\min}^2} - \sqrt{2n - 1}$	12.99	1.537
$P(\chi^2 \geq \chi_{\min}^2)$	$8 \cdot 10^{-39}$	6%

For the fits, amplification values have been used rather than the magnification values as obtained from the OGLE collaboration. These amplification values refer to a baseline, which has been obtained by fitting the tail region to a constant brightness. One obtains also a scaling factor γ , which corresponds to the most-likely size of the errors. Table 3 shows the results.

² In contrast to “merged offset dim” events, there exist two disjoint regions (near the two binary source objects) where the amplification is larger than the detection threshold A_T (usually defined as $A_T = 1.34$) for “offset dim” events.

Table 2. OGLE #5: Binary source fit

parameter	OGLE#5
t_E [d]	$26.3^{+19}_{-3.6}$
$t_{\max,1}$ [d]	$824.359^{+0.018}_{-0.018}$
$t_{\max,2}$ [d]	$827.1^{+73}_{-3.4}$
$u_{\min,1}$	$0.032^{+0.005}_{-0.013}$
$u_{\min,2}$	$0.89^{+0.28}_{-0.19}$
ω	$0.618^{+0.15}_{-0.054}$
m_{base}	$-17.958^{+0.012}_{-0.012}$
χ^2_{\min}	110.58
# d.o.f = n	94
$\sqrt{2\chi^2_{\min} - \sqrt{2n - 1}}$	1.197
$P(\chi^2 \geq \chi^2_{\min})$	12 %

Table 3. OGLE #5: fixing of the baseline and scaling factor γ

parameter	value
begin peak [d]	775
end peak [d]	875
m_{base}	-17.9524
γ	1.503

For the fits of the light curve, the errors have been increased by the factor γ . The need for rescaling arises from the fact that the assumption of a constant tail does not hold for the original data. The error bounds shown correspond to projections of the hypersurface $\Delta\chi^2 = \chi^2 - \chi^2_{\min} = 1$.

Note that the single source fit without blending is not acceptable. The error bounds on t_E are large for the fit with blending: The boundaries of the 1- σ -intervals differ by a factor of 1.5 so that the expectation values for the masses would differ by a factor of about 2.

The differences between the fits with and without blending can be seen in the light curves of the peak region in Fig. 1. The magnitudes are shown as the ordinate, which allows to see the data and the light curve in the peak better, though the fits have been performed using the amplification values. One sees a dramatic improvement of the fit with blending compared with fit without. For the fit without blending, one has many discrepant points in the wings of the light curve, which is not the case for the fit with blending.

The light curve for a binary source (Fig. 1) is similar to that for a single source with blending. The lens passes close to object 1, whereas the minimal separation to the position of object 2 projected onto the lens plane is about 0.7–1.2 r_E . The luminosity offset ratio is ω in agreement with the blending parameter $1 - f$ if one considers the quoted 1- σ -bounds — so that the binary source corresponds to a single source object 1 event

with blending —, the values meet at about 1.2σ . For the binary source fit, there are large uncertainties in the event time scale t_E , the minimal distance to object 2, $u_{\min,2}$, the time of closest approach to object 2, $t_{\max,2}$, and in the luminosity offset ratio ω . The extremely large upper bound on $t_{\max,2}$ is due to the lack of data points for $t > 840$ d, since light curves are possible which involve another peak in this region. However, this bound is not arbitrarily large because this peak still has some influence to the right wing of the peak near $t = 825$ d. If this peak would move to infinity one would approach the fit for a single source with blending which however has a χ^2_{\min} which is larger by about 7.

Figure 2 shows the lens trajectory and the magnification contours for the binary source fit for both the cis- and the trans-configuration. All distances are measured in Einstein radii projected to the source plane r'_E .

This example demonstrates that a blended event can successfully be explained by a binary source model and that the error bounds on the parameters which are convolved into the blending parameter are large. However, since the binary source model corresponds to a “merged offset dim” event which should not occur frequently (around 1 % of the binary source events) it does not show the other direction clearly.

6. Summary and conclusions

I have shown that any event involving a blended single source can also be explained by a (non-blended) binary source and argued that most of the binary source events could be successfully explained by a blended single source. This may explain the lack of events which have been claimed as being due to binary sources. This also shows, that due to the intrinsic similarity of light curves of blended single sources and non-blended binary sources, it is difficult to distinguish between these effects.

Acknowledgements. I would like to thank A. C. Hirshfeld, S. Mao, and C. Alard for reading different versions of the manuscript, the OGLE collaboration for making available their data and an anonymous referee for commenting on some points which helped to clarify them.

References

- Alard C., 1997, A&A 321, 424
- Alard C., Guibert J., Bienayme O., et al., 1995a, The ESO Messenger 80, 31
- Alard C., Mao S., Guibert J., 1995b, A&A 300, L17
- Alcock C., Akerlof C. W. Allsman R. A., et al., 1993, Nat 365, 621
- Alcock C., Allsman R. A., Alves D., et al., 1997a, ApJ 486, 697
- Alcock C., Allsman R. A., Alves D., et al., 1997b, ApJ 479, 119
- Aubourg E., Bareyre P., Bréhin S., et al., 1993, Nat 365, 623
- Bennett D., Alcock C., Allsman R. A., et al., 1996, Nucl. Phys. Proc. Suppl. 51, 152
- Dominik M., 1996, Galactic microlensing beyond the standard model, PhD thesis, Universität Dortmund
- Dominik M., Hirshfeld A.C., 1994, A&A 289, L31
- Dominik M., Hirshfeld A.C., 1996, A&A 313, 841

- Griest K., Hu W., 1992, ApJ, 397, 362 (Erratum: 1993, ApJ 407, 440)
- Pratt M., Marshall S., Alcock C., et al., 1995, BAAS 187, 4706
- Stubbs C., et al. (MACHO collaboration), 1997,
<http://darkstar.astro.washington.edu>
- Udalski A., Szymański M., Kałużny J., et al., 1994a, Acta Astron. 43,
289
- Udalski A., Szymański M., Kałużny J., et al., 1994b, Acta Astron. 44,
227
- Udalski A., Szymański M., Kałużny J., et al., 1994c, Acta Astron. 44,
1
- Udalski A., Szymański M., Mao S., et al., 1994d, ApJ 436, L103
- Udalski A., Szymański M., Stanek K. Z., et al., 1994e, Acta Astron.
44, 165

Fig. 1. OGLE#5: Fit with a single source (top), a blended single source (middle) and a binary source (bottom).

Fig. 2. OGLE#5: Magnification contour plot for the binary source fit and the cis-configuration (left) and the trans-configuration (right) together with the lens trajectory. 9 contours with $\Delta\text{mag} = 0.5 \dots 2.5$ in steps of 0.25.

Figure 1 (top)

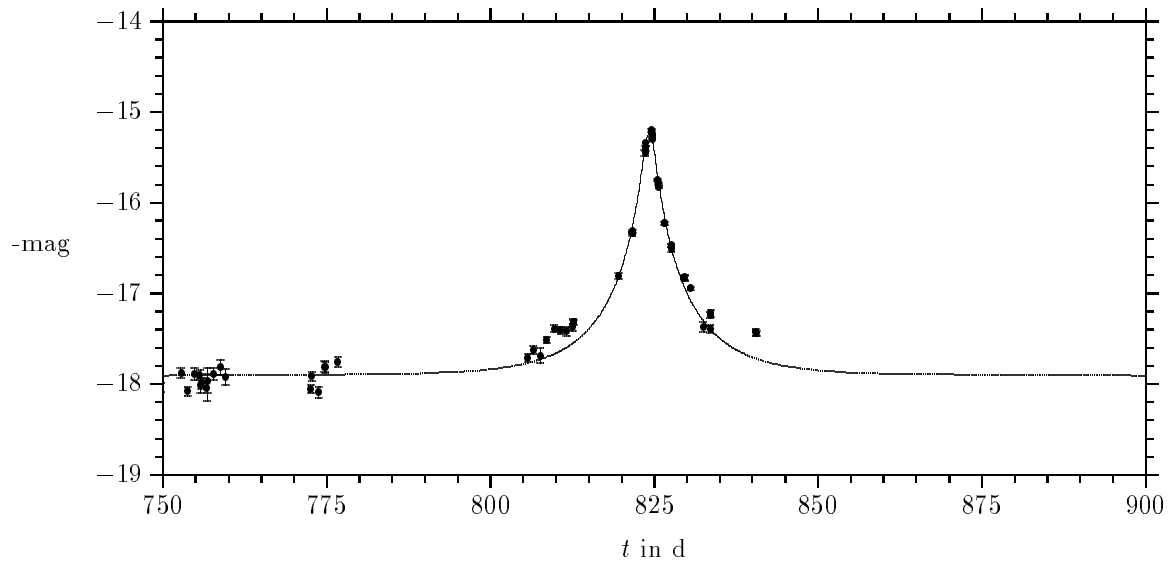


Figure 1 (middle)

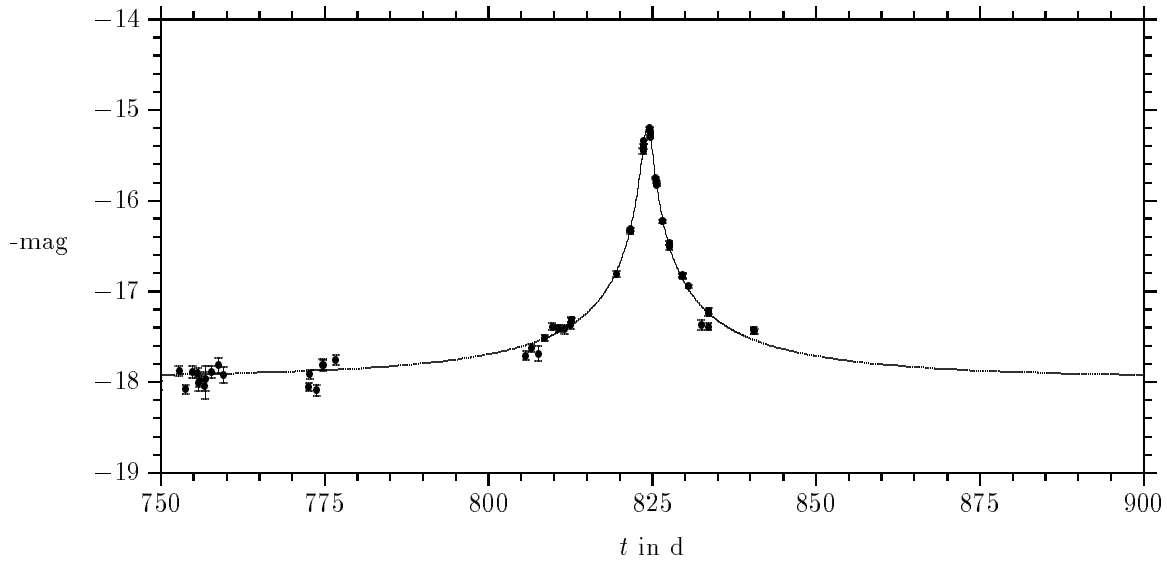


Figure 1 (bottom)

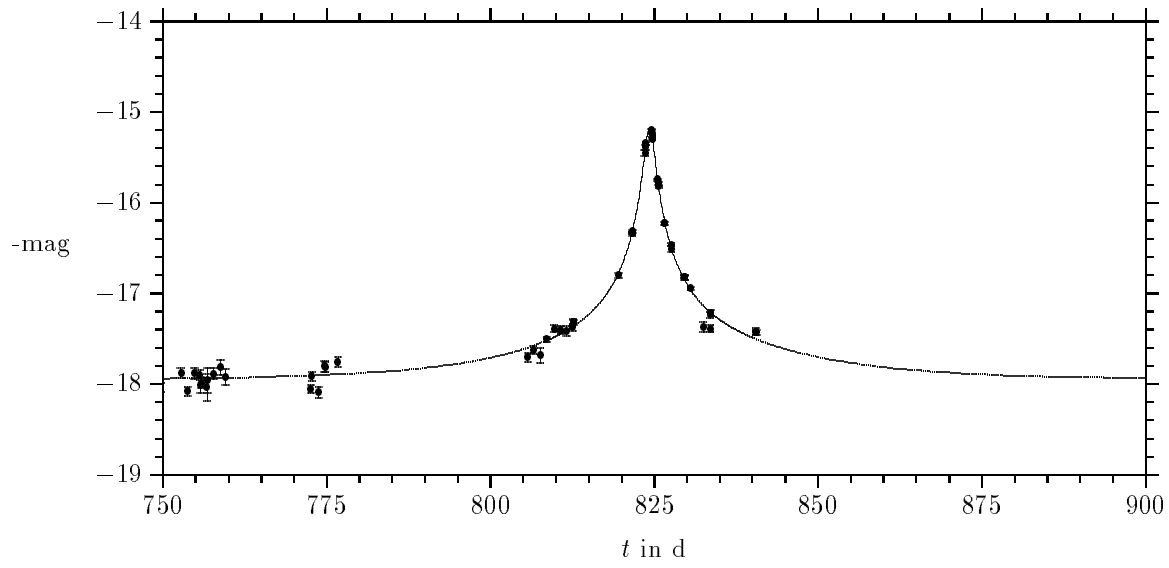


Figure 2 (left)

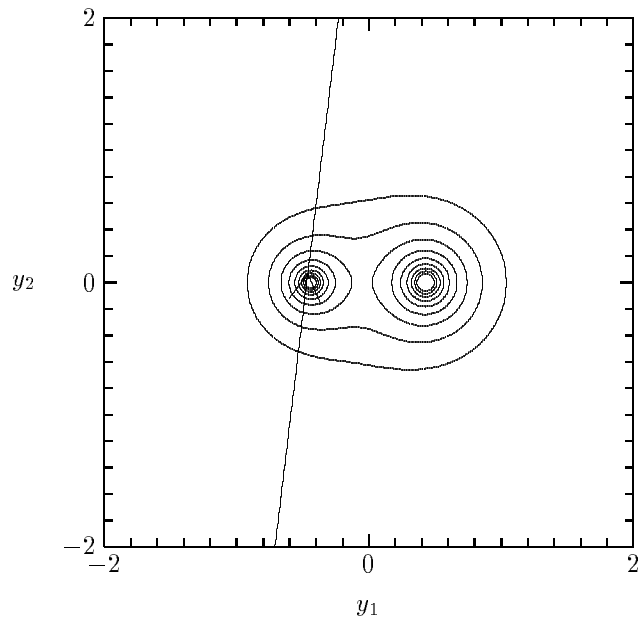


Figure 2 (right)

